Cancer Research

A Novel Anticancer Agent, Decursin, Induces G_1 Arrest and Apoptosis in Human Prostate Carcinoma Cells

Dongsool Yim, Rana P. Singh, Chapla Agarwal, et al.

Updated Version	Access the most recent version of this article at: http://cancerres.aacrjournals.org/content/65/3/1035

Cited Articles	This article cites 38 articles, 9 of which you can access for free at: http://cancerres.aacrjournals.org/content/65/3/1035.full.html#ref-list-1
Citing Articles	This article has been cited by 8 HighWire-hosted articles. Access the articles at: http://cancerres.aacrjournals.org/content/65/3/1035.full.html#related-urls

E-mail alerts	Sign up to receive free email-alerts related to this article or journal.
Reprints and Subscriptions	To order reprints of this article or to subscribe to the journal, contact the AACR Publications Department at pubs@aacr.org.
Permissions	To request permission to re-use all or part of this article, contact the AACR Publications Department at permissions@aacr.org.

A Novel Anticancer Agent, Decursin, Induces G$_1$ Arrest and Apoptosis in Human Prostate Carcinoma Cells

Dongsool Yim,[1] Rana P. Singh,[2] Chapla Agarwal,[2] Sookyeon Lee,[1] Hyungjoon Chi,[4] and Rajesh Agarwal[2,3]

[1]Department of Pharmacy, Sahm Yook University, Seoul, Korea; [2]Department of Pharmaceutical Sciences, School of Pharmacy and [3]University of Colorado Cancer Center, University of Colorado Health Sciences Center, Denver, Colorado; and [4]Natural Product Research Institute, Seoul National University, Seoul, Korea

Abstract

We isolated a coumarin compound decursin (C$_{19}$H$_{20}$O$_5$; molecular weight 328) from Korean angelica (*Angelica gigas*) root and characterized it by spectroscopy. Here, for the first time, we observed that decursin (25-100 μmol/L) treatment for 24 to 96 hours strongly inhibits growth and induces death in human prostate carcinoma DU145, PC-3, and LNCaP cells. Furthermore, we observed that decursinol [where (CH$_3$)$_2$-C=CH-COO- side chain of decursin is substituted with -OH] has much lower effects compared with decursin, suggesting a possible structure-activity relationship. Decursin-induced growth inhibition was associated with a strong G$_1$ arrest ($P < 0.001$) in DU145 and LNCaP cells, and G$_1$, S as well as G$_2$-M arrests depending upon doses and treatment times in PC-3 cells. Comparatively, decursin was nontoxic to human prostate epithelial PWR-1E cells and showed only moderate growth inhibition and G$_1$ arrest. Consistent with G$_1$ arrest in DU145 cells, decursin strongly increased protein levels of Cip1/p21 but showed a moderate increase in Kip1/p27 with a decrease in cyclin-dependent kinases (CDK); CDK2, CDK4, CDK6, and cyclin D1, and inhibited CDK2, CDK4, CDK6, cyclin D1, and cyclin E kinase activity, and increased binding of CDK inhibitor (CDKI) with CDK. Decursin-caused cell death was associated with an increase in apoptosis ($P < 0.05$-0.001) and cleaved caspase-9, caspase-3, and poly(ADP-ribose) polymerase; however, pretreatment with all-caspases inhibitor (z-VAD-fmk) only partially reversed decursin-induced apoptosis, suggesting the involvement of both caspase-dependent and caspase-independent pathways. These findings suggest the novel anticancer efficacy of decursin mediated via induction of cell cycle arrest and apoptosis selectively in human prostate carcinoma cells. (Cancer Res 2005; 65(3): 1035-44)

Introduction

Prostate cancer is the most common cancer as well as the second leading cause of cancer-related deaths in men in Western countries (1). One out of nine men over 65 years of age is frequently diagnosed with prostate cancer in the United States (1, 2). Dietary pattern has been identified as one of the major factors for the difference in prostate cancer incidence between Western and Asian countries (2–4). At present, there is no effective therapy available for the treatment of androgen-independent stage of prostate cancer, which usually arises after hormonal deprivation/ablation therapy (5). Cytotoxic chemotherapies or radiotherapy also do not show any significant improvement in patient condition due to the high recurrence of apoptosis resistance hormone refractory prostate cancer, which is responsible for ∼28,000 deaths per year (1, 6, 7). The clinical impact of advanced prostate cancer has led to the exploration of novel treatment modalities as well as anticancer agents. In this regard, many nutritive and nonnutritive phytochemicals with diversified pharmacologic properties have shown promising responses for the prevention and/or intervention of various cancers, including prostate cancer (reviewed in refs. 2–4). In addition, epidemiologic studies, together with extensive basic laboratory findings, support the potential role of phytochemicals in the prevention and treatment of prostate cancer (reviewed in refs. 8–14).

Herbal medicines including conventional and complimentary medicines are still prevalent, and serve the medicinal needs of a large population around the world (reviewed in refs. 15, 16), which could be assessed by the fact that the global herbal medicine market is currently worth around $30 billion. Herbal medicine practice can be traced back to the origin of human culture, having been mentioned in medical protocols such as traditional Chinese medicine and Indian Ayurvedic herbal medicine. At present, there is an increased effort for the isolation of bioactive microchemicals from medicinal plants for their possible usefulness in the control of various ailments. Determining molecular structure and mechanisms of action of bioactive phytochemicals are equally important for providing the evidence for their efficacy as well as herbal preparations, which could also potentially lead to the pharmaceutical development of synthetic or semisynthetic drugs.

Angelica gigas Nakai (Umbelliferae) root has been traditionally used in Korean folk medicine as a tonic and for treating anemia and other common diseases (17). There are some reports about the pharmacologic evaluation of this plant showing antibacterial and antiamnestic effects, inhibitory effect on acetylcholinesterase, depression of cardiac contraction, activation of protein kinase C, and antitumor activity against sarcoma cancer cells (18–21). Based on the curative potential, efforts have been made to isolate the active principle from this plant, which led to the isolation of many coumarin compounds (22). However, there is no report on the evaluation of anticancer activity of these compounds against epithelial cancers. In the present investigation, we used the roots of *A. gigas* to isolate decursin and decursinol, and for the first time tested their efficacy against human prostate carcinoma cells. A structure-activity relationship was observed for these compounds, with decursin showing greater efficacy in inhibiting growth and causing death of DU145 cells. The anticancer efficacy of decursin was also evident against human prostate cancer PC-3

and LNCaP cells. Furthermore, we investigated the mechanistic rationale for the observed efficacy of decursin, which showed an arrest in cell cycle progression and apoptosis induction as the most likely targets in prostate cancer cells.

Materials and Methods

Plant Material, Isolation and Characterization of Decursin and Decursinol. The roots of *A. gigas* Nakai (family Umbelliferae) were verified by Professor Emeritus Hyungjoon Chi (one of the authors in the present manuscript). The extraction and fractionation of air-dried powdered root was done as reported recently (22). Silica gel column chromatography was used to isolate decursin and decursinol (22). These compounds were characterized by nuclear magnetic resonance (Bruker AVANCE 400 NMR spectrometer) and mass spectroscopy (by Jeol JMS-AX505-WA mass spectrometer) at Natural Product Research Institute, Seoul National University, Seoul, Korea. The purified coumarin compounds, decursin ($C_{19}H_{20}O_5$) with a molecular weight of 328 (Fig. 1*A*), and decursinol ($C_{14}H_{14}O_4$) with a molecular weight of 246 (Fig. 1*B*), were dissolved in DMSO as stock solutions, and used directly in the cell culture treatments.

Cell Line and Reagents. Human prostate carcinoma cell lines DU145, PC-3 and LNCaP, and nonneoplastic human prostate epithelial cell line PWR-1E were obtained from American Type Culture Collection (Manassas, VA). Prostate cancer cells were cultured in RPMI 1640 with 10% fetal bovine serum (Hyclone, Logan, UT) under standard culture conditions (37°C, 95% humidified air, and 5% CO_2). PWR-1E cells were cultured in keratinocyte growth medium supplemented with 10% fetal bovine serum, 5 ng/mL human recombinant epidermal growth factor and 0.05 mg/mL bovine pituitary extract (American Type Culture Collection). RPMI 1640 and other culture materials were from Life Technologies, Inc. (Gaithersburg, MD). Anti-Cip1/p21 antibody was from Calbiochem (Cambridge, MA), and anti-Kip1/p27 antibody was from Neomarkers, Inc. (Fremont, CA). Antibodies to cyclin-dependent kinase (CDK); CDK2, CDK4, and CDK6, cyclin D1 and E, and Rb-glutathione *S*-transferase fusion protein were from Santa Cruz Biotechnology, Inc. (Santa Cruz, CA). Anti-caspases primary antibodies and anti-cleaved poly(ADP-ribose) polymerase (PARP) antibody were from Cell Signaling Technology (Beverly, MA). Anti-total PARP antibody was from BD PharMingen (San Diego, CA). Histone H1 was from Boehringer Mannheim, Corp. (Indianapolis, IN). [γ-^{32}P] ATP (specific activity 3,000 Ci/mmol) and enhanced chemiluminescence (Amersham) detection system were from Amersham Corp. (Piscataway, NJ). Other chemicals were obtained in their commercially available highest purity grade.

Cell Growth and Death Assays. Cells were plated at 5,000 cells/cm^2 in 60 mm plates under the standard culture conditions detailed above and after 24 hours, fed with fresh medium and treated with DMSO control or 25, 50, and 100 μmol/L decursin or decursinol. After the desired treatment time, cells were collected by a brief trypsinization, and counted in duplicate with a hemocytometer using Trypan blue dye to score dead cells. Each treatment and time point had three independent plates. The representative data shown in this study were reproducible in three independent experiments.

Cell Cycle Analysis by Flow Cytometry. Prostate cancer cells and PWR-1E cells were grown in 10% serum condition in their respective culture mediums as mentioned above. At ∼30% confluency, cells were treated with DMSO control or 25, 50, and 100 μmol/L decursin and at the end of desired treatment time, cells were collected and processed for cell cycle analysis. Briefly, 0.5×10^5 cells were suspended in 0.5 mL of saponin/propidium iodide solution [0.3% saponin (w/v), 25 μg/mL propidium iodide (w/v), 0.1 mmol EDTA, and 10 μg/mL RNase (w/v) in PBS], and incubated overnight at 4°C in the dark. Cell cycle distribution was then analyzed by flow cytometry using fluorescence-activated cell sorting core facility of University of Colorado Cancer Center. Finally, the percentage of cells in different phases of cell cycle were determined by ModFit LT cell cycle analysis software.

Immunoblotting and Immunoprecipitation. DU145 cells were grown in RPMI 1640 medium and treated with DMSO control or 25, 50, and 100 μmol/L decursin for the desired times. Equal volumes of DMSO (0.1% v/v) were present in each treatment. Following decursin treat-

ments, cell lysates were prepared in nondenaturing lysis buffer [10 mmol Tris-HCl (pH 7.4), 150 mmol NaCl, 1% Triton X-100, 1 mmol EDTA, 1 mmol EGTA, 0.3 mmol phenylmethylsulfonyl fluoride, 0.2 mmol sodium orthovanadate, 0.5% NP40, and 5 units/mL aprotinin]. For lysate preparation, medium was aspirated and cells were washed twice with ice-cold PBS followed by incubation in lysis buffer for 20 minutes. Then, cells were scraped and kept on ice for an additional 30 minutes, and finally cell lysates were cleared by centrifugation at 4°C for 30 minutes in a tabletop centrifuge. Protein concentration in lysates was determined using Bio-Rad detergent-compatible protein assay kit (Bio-Rad Laboratories, Hercules, CA) by Lowry method.

For Western blotting, 60 to 80 μg of protein lysate per sample was denatured in 2× SDS-PAGE sample buffer and subjected to SDS-PAGE on 12% or 16% tris-glycine gel as published recently (23). The separated proteins were transferred on to nitrocellulose membrane followed by blocking of membrane with 5% nonfat milk powder (w/v) in TBS (10 mmol Tris, 100 mmol NaCl, 0.1% Tween 20) for 1 hour at room temperature or overnight at 4°C. Membranes were probed for the protein levels of Cip1/p21, Kip1/p27, CDK2, CDK4, CDK6, cyclin D1, and E using specific primary antibodies followed by peroxidase-conjugated appropriate secondary antibody, and visualized by enhanced chemiluminescence (Amersham) detection system. Similarly, for apoptotic molecules, cleaved caspase-9, cleaved caspase-3, total PARP and cleaved PARP were probed using their specific primary antibodies followed by appropriate secondary antibody and enhanced chemiluminescence visualization. Membranes were stripped and reprobed with β-actin primary antibody as a protein loading control.

For CDK inhibitor (CDKI)-CDK binding study, DU145 cells were treated with 100 μmol/L decursin for 24 hours and whole cell lysates were prepared. For each sample, 200 μg protein lysates was cleared with protein A/G-plus agarose beads (Santa Cruz) for 45 minutes at 4°C. Cip1/p21 and Kip1/p27 were then immunoprecipitated from protein lysates using specific antibody (2 μg) incubation for 6 hours followed by addition of 25 μL of protein A/G-plus agarose beads and rocking overnight at 4°C. Immunoprecipitates were washed thrice with lysis buffer, and samples were boiled in 2× sample buffer for 5 minutes followed by centrifugation. The resulting clear supernatants were subjected to SDS-PAGE on 16% gel and Western blotting. Membranes were then probed with and visualized for CDK2, CDK4, and CDK6 as detailed above.

Kinase Assays. CDK2 and cyclin E-associated histone H1 kinase activity was determined as described recently (23). Briefly, 200 μg of protein lysates from each sample was precleared with protein A/G-plus agarose beads, and CDK2 and cyclin E proteins were immunoprecipitated using anti-CDK2 and anti–cyclin E antibodies (2 μg) and protein A/G-plus agarose beads, respectively. Beads were washed thrice with lysis buffer, and finally with kinase assay buffer [50 mmol Tris-HCl (pH 7.4), 10 mmol $MgCl_2$ and 1 mmol DTT]. Phosphorylation of histone H1 was measured by incubating the beads with 30 μL of "hot" kinase solution [0.25 μL (2.5 μg) of histone H1, 0.5 μL (5 μCi) of γ-^{32}P-ATP, 0.5 μL of 0.1 mmol ATP, and 28.75 μL of kinase buffer] for 30 minutes at 37°C. The reaction was stopped by boiling the samples in SDS sample buffer for 5 minutes. The samples were then subjected to 12% SDS-PAGE, and the gel was dried and analyzed by autoradiography (23). Similarly, to determine CDK4, CDK6, and cyclin D1-associated Rb kinase activities, these proteins were immunoprecipitated using specific antibodies, and beads conjugated with antibody and proteins were washed thrice with Rb-lysis buffer [50 mmol HEPES-KOH (pH 7.5), 150 mmol NaCl, 1 mmol EDTA, 2.5 mmol EGTA, 1 mmol DTT, 80 mmol β-glycerophosphate, 1 mmol NaF, 0.1 mmol sodium orthovanadate, 0.1% Tween 20, 10% glycerol, 1 mmol phenylmethylsulfonyl fluoride, and 10 μg/mL leupeptin and aprotinin] and twice with Rb-kinase assay buffer [50 mmol HEPES-KOH (pH 7.5), 2.5 mmol EGTA, 10 mmol β-glycerophosphate, 1 mmol NaF, 10 mmol $MgCl_2$, 0.1 mmol sodium orthovanadate, and 1 mmol DTT]. Phosphorylation of Rb was measured by incubating the beads with 30 μL of hot Rb-kinase solution (2 μg of Rb-glutathione *S*-transferase fusion
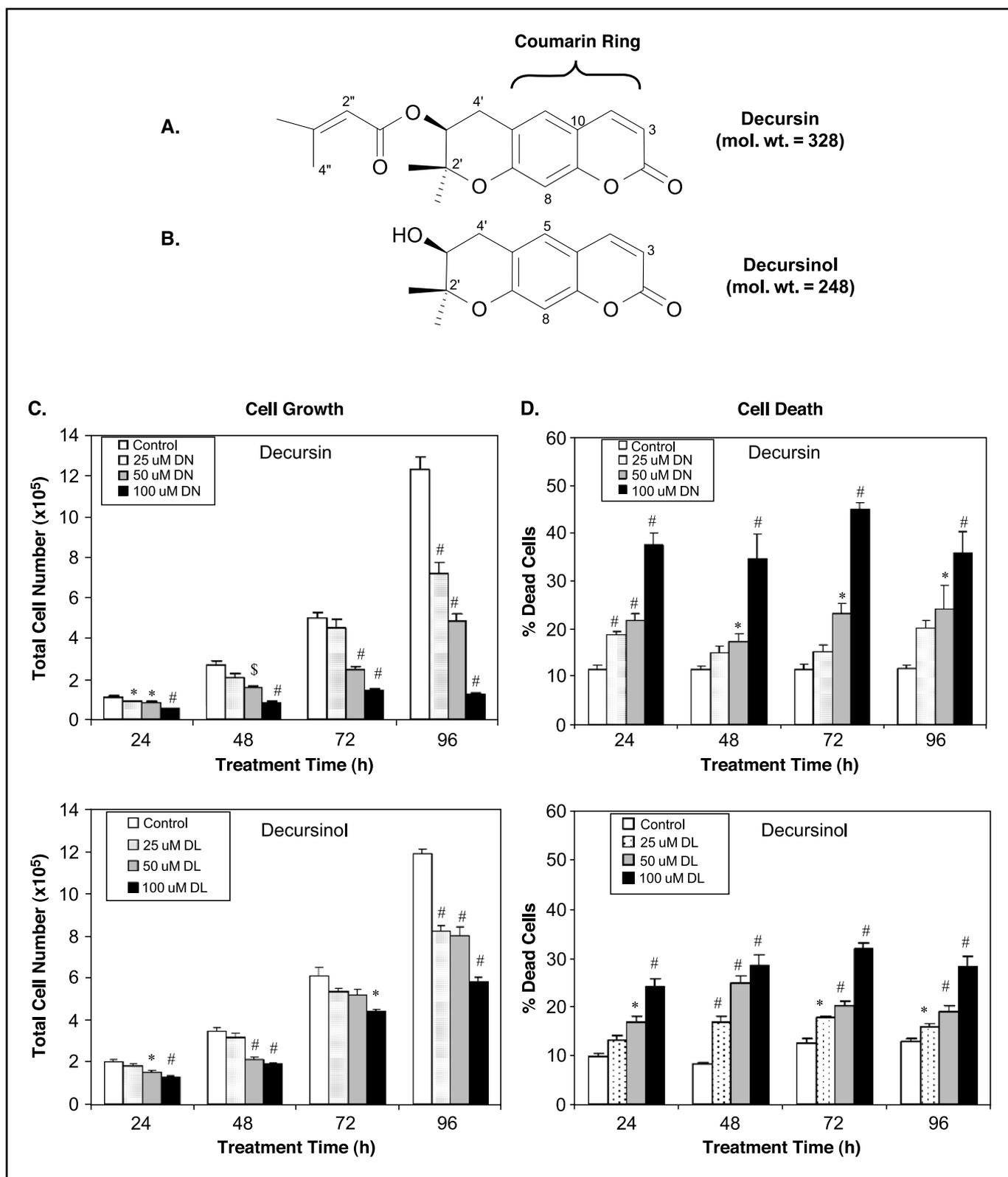
Figure 1. Structure, growth inhibitory, and cell death effects of decursin and decursinol on DU145 cells. Chemical structure of decursin (*A*) and decursinol (*B*), isolated from the roots of *A. gigas*. To assess the effect of decursin and decursinol on exponentially growing DU145 cells, 5,000 cells/cm^2 were plated in 60 mm dishes and the next day, cells were treated either DMSO vehicle control or 25, 50, and 100 μmol/L doses of decursin or decursinol in complete medium. After 24, 48, 72, and 96 hours of these treatments, total cells were counted using a hemocytometer (*C*), dead cells were scored using Trypan blue dye exclusion method (*D*). Mean ± SE of three independent plates; each sample was counted in duplicate. *DN*, decursin; *DL*, decursinol; *, $P < 0.05$; $^\$$, $P < 0.01$; #, $P < 0.001$ versus control.

protein, 5 μCi of γ-^{32}P-ATP, and 0.1 mmol ATP in Rb-kinase buffer) for 30 minutes at 37°C. Reaction was stopped by boiling the samples in 5× SDS sample buffer for 5 minutes. Samples were analyzed by SDS-PAGE, and the gel was dried and subjected to autoradiography (23).

Apoptotic Cell Death Assay. To quantify decursin-induced apoptotic death of human prostate carcinoma DU145 cells, annexin V, and propidium iodide staining was done followed by flow cytometry, as described recently (23, 24). Briefly, after treatment (DMSO control, 50 and 100 μmol/L decursin for 24 and 48 hours), cells were collected and subjected to annexin V and propidium iodide staining using Vybrant Apoptosis Assay Kit2 (Molecular Probes, Inc., Eugene, OR) and following the step-by-step protocol provided by the manufacturer. Annexin V binds to phospatidylserine, which is translocated from inner to outer leaflet of the plasma membrane in apoptotic cells. In all-caspases inhibitor (z-VAD-fmk; Enzyme Systems Products, ICN Pharmaceuticals, Inc., Aurora, OH) treatment, cells were pretreated with the inhibitor for 2 hours before decursin treatment.

Caspase Activity Assay. Caspase-3 activity was assayed by colorimetric protease assay ApoTarget kit (BioSource International, Inc., CA) following manufacturer's protocol as published recently (24). Briefly, at the end of treatment with either 100 μmol/L dose of decursin, or all-caspases inhibitor z-VAD-fmk (100 μmol/L), or both, in which cells were pretreated for a total of 48 hours with the inhibitor for 2 hours, cells were collected and cell lysates prepared in cell lysis buffer (TBS containing detergent). Protein lysate (100 μg per sample) was mixed with 2× reaction buffer and 200 μmol/L substrate (DEVD-pNA for caspase-3) and incubated at 37°C for 3 hours in the dark. These assay conditions are standardized and products of the reaction remain in the linear range of detection. Developed color was measured at 405 nm in microplate reader, and blank reading was subtracted from each sample reading before calculation.

Statistical Analysis. The data were analyzed using the Jandel Scientific SigmaStat 2.03 software. Student's *t* test was employed to assess the statistical significance of difference between control and decursin-treated or decursinol-treated groups. A statistically significant difference was considered to be present at $P < 0.05$. Autoradiograms/bands were scanned with Adobe Photoshop 6.0 (Adobe Systems, Inc. San Jose, CA).

Results

Nuclear Magnetic Resonance and Mass Characterization of Decursin and Decursinol. Decursin: white crystals from CH$_3$OH. [^{1}H] NMR (400 MHz, CDCl$_3$) δ$_H$ (ppm): 7.57 (1H, d, J = 9.5 Hz, H-4), 7.14 (1H, s, H-5), 6.78 (1H, s, H-8), 6.21 (1H, d, J = 9.5 Hz, H-3), 5.64 (1H, s, H-2′), 5.06 (1H, t, J = 4.6 Hz, H-3′), 3.17 (1H, dd, J = 16.0, 4.2 Hz, H-4′$_a$), 2.85 (1H, dd, J = 16.0, 4.2 Hz, H-4′$_b$), 2.12 (3H, s, 3′-CH$_3$), 1.86 (3H, s, H-4″), 1.36 (3H, s, *gem*-CH$_3$), 1.34 (3H, s, *gem*-CH$_3$). Fast atom bombardment mass spectroscopy: *m/z* (rel. int., %): 329 (100) [M + H]$^+$, 228 (100), 213 (95), 154 (45), 136 (45; Fig. 1*A*). Decursinol: white crystals from CH$_3$OH. [^{1}H] NMR (400 MHz, CDCl$_3$) $_H$ (ppm): 7.57 (1H, d, J = 9.5 Hz, H-4), 7.17 (1H, s, H-5), 6.77 (1H, s, H-8), 6.21 (1 H, d, J = 9.2 Hz, H-3), 3.86 (1H, t, J = 4.8 Hz, H-3′), 3.10 (1H, dd, J = 17.0, 4.5 Hz, H-4′$_a$) 2.83 (1H, dd, J = 17.0, 4.5 Hz, H-4′$_b$) 1.39 (3H, s, *gem*-CH$_3$), 1.36 (3H, s, *gem*-CH$_3$). Fast atom bombardment mass spectroscopy: *m/z* (rel. int., %): 247 (100) [M + H]$^+$, 246 (85), 154 (100), 136 (90; Fig. 1*B*).

Effects of Decursin and Decursinol on Growth and Death of DU145 Cells. To assess the biological activity of these compounds in terms of cell growth and death, DU145 cells were treated with 25, 50, and 100 μmol/L doses of decursin and decursinol for 24, 48, 72, and 96 hours. Decursin (25-100 μmol/L) showed a strong dose- and time-dependent inhibition of cell growth, accounting for 22% to 51% ($P < 0.05$-0.001), 21% to 68% ($P < 0.01$-0.001), 9% to 72% ($P < 0.001$), and 42% to 90% ($P < 0.001$) growth inhibition after 24, 48, 72, and 96 hours of treatment, respectively (Fig. 1*C*). However, similar treatment with decursinol (25-50 μmol/L for 24, 48, 72, and 96 hours) showed

almost half the efficacy of decursin, accounting for 11% to 36% ($P < 0.05$-0.001), 9% to 45% ($P < 0.01$-0.001), 9% to 27% ($P < 0.001$), and 31% to 51% ($P < 0.001$) growth inhibition, respectively (Fig. 1*C*). These data suggest that decursin is much more potent in inhibiting the growth of DU145 as compared with decursinol. The differences in biological activity of these two compounds could be attributed to the difference in their chemical structures (Fig. 1*A* and *B*). The increased activity of decursin could be, most likely, due to (CH$_3$)$_2$-C=CH-COO- side chain of decursin which is substituted with OH group in decursinol (Fig. 1*A* and *B*). Furthermore, we observed that both compounds have cytotoxic effect on DU145 cells, in which similar treatment (25-100 μmol/L for 24, 48, 72, and 96 hours) with decursin caused 15% to 45% ($P < 0.05$-0.001) cell death versus 11% to 12% in controls (Fig. 1*D*), whereas decursinol caused 13% to 32% ($P < 0.05$-0.001) cell death as compared with 8% to 13% in controls (Fig. 1*D*). When these cytotoxicity data were compared between these two agents, at similar doses and treatment times, decursin showed a relatively better cell death effect compared with decursinol, except at 48 hours of treatment; however, it was statistically significant (decursin versus decursinol) only at 25 μmol/L dose for 96-hour ($P < 0.05$) and 100 μmol/L dose for 72-hour ($P < 0.001$) treatments. These data suggest a relatively higher cytotoxic effect of decursin as compared with decursinol, and further support a possible structure-activity relationship in their overall effects in DU145 cells. Next, we investigated the growth inhibitory and cytotoxic effects of decursin on human prostate cancer PC-3 and LNCaP cells, and human prostate epithelial PWR-1E cells, and mechanisms associated with these effects of decursin in DU145 cells.

Effect of Decursin on Growth and Death of Human Prostate Cancer PC-3 and LNCaP Cells, and Human Prostate Epithelial PWR-1E Cells. As compared with DU145 cells, decursin (25-100 μmol/L) treatment of PC-3 cells for 24, 48, 72, and 96 hours, showed stronger dose- and time-dependent growth inhibitory effect accounting for 7% to 54% ($P < 0.05$-0.001), 25% to 75% ($P < 0.05$-0.001), 36% to 84% ($P < 0.05$-0.001), and 49% to 91% ($P < 0.05$-0.001) inhibition, respectively (Fig. 2*A*). However, cytotoxic effect of decursin in PC-3 cells was limited to higher doses only, showing 3% to 18% ($P > 0.05$ to < 0.05-0.001) dead cells as compared with 2% to 5% in controls (Fig. 2*A*). The growth inhibitory effect of decursin in LNCaP cells was stronger than both DU145 and PC-3 cells. In similar decursin treatment for 24, 48, 72, and 96 hours, 9% to 72% ($P > 0.05$ to < 0.005-0.001), 48% to 83% ($P < 0.005$-0.001), 76% to 94% ($P < 0.001$), and 79% to 98% ($P < 0.001$) cell growth inhibition was observed in LNCaP cells, respectively (Fig. 2*B*). The cytotoxic effect of decursin in LNCaP cells was also greater than that of DU145 and PC-3 cells accounting for 16% to 52% ($P > 0.05$ to < 0.05-0.001) cell death as compared with 8% to 16% in controls (Fig. 2*B*). Overall, these results suggested growth inhibitory and cytotoxic effects of decursin in human prostate carcinoma PC-3, LNCaP as well as DU145 cells.

Furthermore, using nonneoplastic human prostate epithelial PWR-1E cells, we assessed whether decursin has any differential sensitivity to normal versus cancer cells. Surprisingly, we did not observe any increase in dead cells following decursin treatment; it was even significantly lower ($P < 0.05$ versus control) following 72 hours of treatment at the 100 μmol/L dose (Fig. 2*C*). A decrease in cell number, however, was observed after decursin treatment of PWR-1E cells, but it was not as strong as in the case of prostate carcinoma cells (Fig. 2*C*). For instance, growth
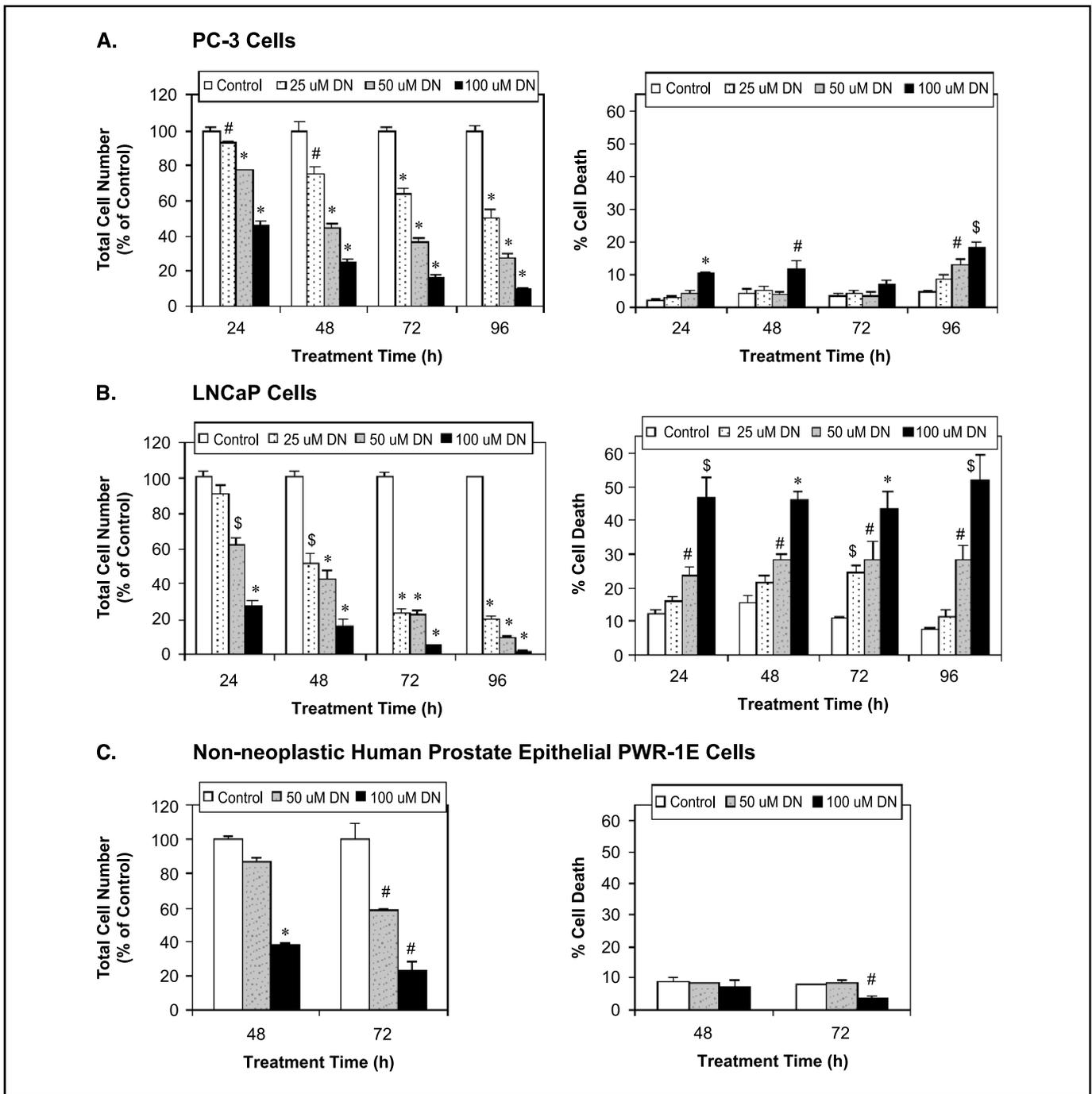
Figure 2. Growth inhibitory and cell death effects of decursin on PC-3, LNCaP, and PWR-1E cells. To assess the effect of decursin on exponentially growing human PCA PC-3 (*A*), LNCaP (*B*) cells, and nonneoplastic prostate epithelial PWR-1E cells (*C*), 5,000 cells/cm² were plated in 60 mm dishes and the next day, cells were treated either DMSO vehicle control or 25, 50, and 100 μmol/L doses of decursin in complete medium. After the indicated treatment times, total cells were counted using a hemocytometer, and dead cells were scored using Trypan blue dye exclusion method. Mean ± SE of three independent plates; each sample was counted in duplicate. *DN*, decursin; *DL*, decursinol; *, *P* < 0.05; $, *P* < 0.01; #, *P* < 0.001 versus control.

inhibition caused by 50 to 100 μmol/L doses of decursin was 56% to 75% (48 hours) and 64% to 84% (72 hours) in PC-3 cells; and 58% to 83% (48 hours) and 77% to 94% (72 hours) in LNCaP cells as compared with 14% to 62% (48 hours) and 41% to 77% (72 hours) in PWR-1E cells (Fig. 2). After 24 hours of decursin treatment, we did not observe any considerable growth inhibition or cell death in PWR-1E cells (data not shown).

These results suggest that decursin is not toxic to prostate epithelial cells; however, it inhibits their growth with lesser efficacy as compared with cancer cells in culture.

Decursin Induces a Strong G₁ Arrest in Cell Cycle Progression of Prostate Cancer Cells. Inhibition of deregulated cell cycle progression in cancer cells is an effective strategy to halt tumor growth (14, 25). Because we observed a strong growth

inhibitory effect of decursin, we then analyzed its possible inhibitory effect on cell cycle progression following 25, 50, and 100 μmol/L doses of decursin treatment for 12 to 96 hours. We observed that decursin induces G_1 arrest, which started as early as 12 hours after the treatment in DU145 cells (data not shown). An optimum dose-dependent effect was observed at 24 hours of treatment where decursin caused 52%, 65%, and 78% DU145 cells in G_1 phase ($P < 0.001$) as compared with 45% in control (Fig. 3A and B); this effect started diminishing after 48 hours of treatment (data not shown). An increase in G_1 cell population was mostly at the expense of S phase cells ($P < 0.05$-0.01) with a minimal decrease in G_2-M cell population (Fig. 3B).

Similarly, in PC-3 cells, a strong G_1 arrest was observed at 25 and 50 μmol/L decursin treatment for 24 hours (Fig. 4A), which started diminishing at later treatment times leading to a moderate G_2-M arrest (data not shown). However, 100 μmol/L dose of decursin invariably showed an increase in S and/or G_2-M phase cell population in PC-3 cells at all treatment times (Fig. 4A; data for later treatment times not shown). Similar to DU145 and PC-3 cells, decursin (25-50 μmol/L) caused significant increase in G_1 cell population at the expense of S as well as G_2-M phase cell populations in LNCaP cells (Fig. 4B). However, in contrast to DU145 and PC-3 cells, this effect of decursin in LNCaP cells did not diminish and remained sustained even at 96 hours of the treatment (data not shown). Higher doses (100 μmol/L) of decursin, interestingly, showed a time-dependent increase in G_1 arrest in LNCaP cells (data not shown). Furthermore, in nonneoplastic prostate epithelial PWR-1E cells, only a moderate increase in G_1 arrest was observed only at higher doses (100 μmol/L) of decursin treatment (Fig. 4C). However, both lower doses (25 and 50 μmol/L) that were effective in prostate cancer cells did not show any cell cycle effect in PWR-1E cells (Fig. 4C; and data not shown). These results suggest that inhibition of deregulated cell cycle progression could be one of the molecular events associated with selective anticancer efficacy of decursin in prostate cancer cells.

Decursin Up-regulates Cip1/p21 and Kip1/p27 Levels, and Inhibits CDK- and Cyclin-Associated Kinase Activity. Since, we observed optimum G_1 cell cycle arrest by decursin at 24 hours in DU145 cells, and a relatively similar effect at 48 hours (data

not shown), total cell lysates were prepared following decursin treatment of cells at 25, 50, and 100 μmol/L doses for 24 and 48 hours. Western blot analysis of total cell lysates (80 μg/sample) showed a strong dose-dependent increase in the expression of Cip1/p21, which was moderate in case of Kip1/p27 (Fig. 5A). Reprobing of membranes for β-actin confirmed equal protein loading (Fig. 5A, *bottom*). In the studies analyzing its effect on the levels of CDKs and cyclins associated with G_1 phase, decursin treatment for 24 hours did not show any alteration in protein levels of CDK2, CDK4, CDK6, cyclin D1, and cyclin E; however, 48 hours of treatment showed a dose-dependent decrease in the expression of these proteins except cyclin E (Fig. 5B).

Next, cell lysates were assayed for CDK2, CDK4, CDK6, cyclin D1, and cyclin E kinase activity. As shown in Fig. 5C, compared with control, decursin treatment resulted in almost complete inhibition in CDK2, cyclin E, and cyclin D1 kinase activity; however, the inhibitory effect of decursin on CDK4- and CDK6-associated kinase activity was of lower magnitude (Fig. 5C). We anticipated that the observed inhibition in kinase activity of these CDKs and cyclins could in part be due to an up-regulated level of CDKIs and their binding with CDK-cyclin complex, causing a resultant G_1 arrest. To support this anticipation, we immunoprecipitated Cip1/p21 and Kip1/p21 from total cell lysates, and studied their binding with CDK2, CDK4, and CDK6, which showed an increase in the bound levels of these proteins following decursin treatment (Fig. 5D). These results suggest a possible increase in CDK-cyclin-CDKI complex formation accompanied by a decrease in CDK kinase activity following decursin treatment.

Decursin Induces Apoptotic Death of DU145 Cells. During cell growth assay, we observed that decursin causes a significant increase in DU145 cell death, where higher doses and longer treatment times were more effective. Here, using annexin V-staining and flow cytometry, we assessed whether decursin-caused cell death is mediated by apoptosis. Cells were treated with DMSO control, 50, and 100 μmol/L doses of decursin for 24 and 48 hours for the apoptosis analysis. Our data show a dose-dependent increase (up to ∼3-fold, $P < 0.05$-0.001) in apoptotic cell population following decursin treatment (Fig. 6A). Lower doses (50 μmol/L) of
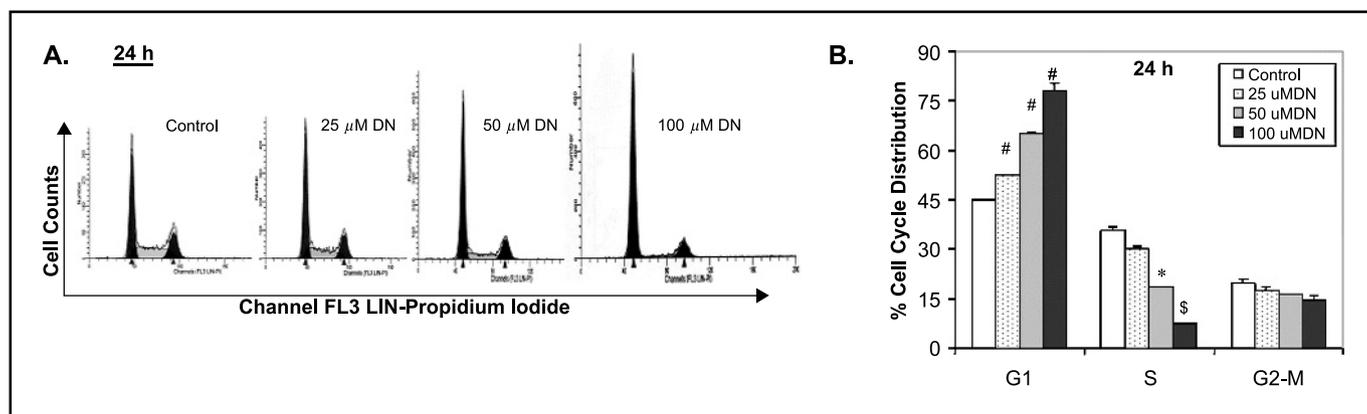
Figure 3. Effect of decursin on cell cycle progression in DU145 cells. Cells were cultured in complete medium, and treated with either DMSO vehicle control or 25 to 100 μmol/L doses of decursin. After 24 hours of these treatments, cells were collected, washed with PBS, digested with RNase, and then cellular DNA was stained with propidium iodide as detailed in Materials and Methods. Flow cytometric analysis was then performed for cell cycle distribution. *A,* propidium iodide fluorescence pattern for cell cycle distribution in different treatments. *B,* the percentage of cell cycle distribution data for each treatment group. Mean ± SE of three independent samples. *DN,* decursin; *, $P < 0.05$; $, $P < 0.01$; #, $P < 0.001$ versus control.
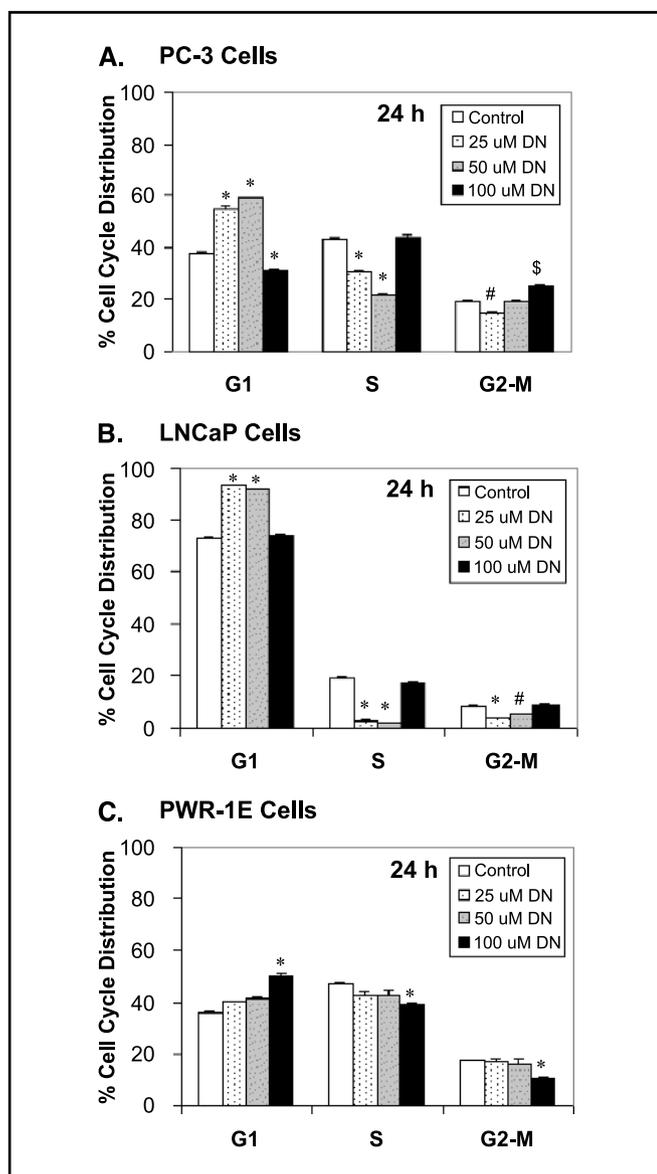
Figure 4. Effect of decursin on cell cycle progression in PC-3, LNCaP, and PWR-1E cells. Cells were cultured in complete medium, and treated with either DMSO vehicle control or 25 to 100 μmol/L doses of decursin. After 24 hours of these treatments, cells were processed and analyzed by flow cytometry as mentioned in Fig. 3. The percentage of cell cycle distribution data for PC-3 (*A*), LNCaP (*B*), and PWR-1E (*C*) cells are shown as mean ± SE of three independent samples. *DN*, decursin; *, $P < 0.05$; $, $P < 0.01$; #, $P < 0.001$ versus control.

we analyzed the levels of cleaved caspase-9 and caspase-3 following 48 hours of treatment. Cleavage of caspases is directly related to their activation status. Our data show that decursin caused an increase in cleaved caspase-9 and caspase-3, which were very prominent at 100 μmol/L dose of decursin (Fig. 6*B*, rows *1* and *2*). Consistent with the cleavage of caspases, decursin also caused a strong increase in PARP cleavage (Fig. 6*B*). First, we used PARP antibody (BD PharMingen) which recognizes both total (116 kDa) as well as cleaved PARP (89 kDa; Fig. 6*B*, row *3*); and later the same membrane was stripped and reprobed with specific cleaved PARP antibody (Cell Signaling) which showed better sensitivity for the detection of cleaved PARP fragment (Fig. 6*B*, row *4*). Furthermore, these membranes were also checked for the level of β-actin as a loading control; only a representative blot is shown in Fig. 6*B* (row *5*).

To further establish the role of caspase activation in decursin-caused apoptosis, we used all-caspases inhibitor z-VAD-fmk (2 hours pretreatment), which only partially reversed the decursin-induced apoptosis (Fig. 6*C*). To confirm whether the dose of all-caspases inhibitor used in the study was sufficient to inhibit caspase activity, caspase-3 activity was also measured under identical treatments. As shown in Fig. 6*D*, 100 μmol/L dose of caspase inhibitor completely inhibited 100 μmol/L decursin-induced (~3 fold) caspase-3 activity. Overall, these results suggested the involvement of both caspase-dependent and caspase-independent pathway(s) in decursin-induced apoptotic death of DU145 cells.

Discussion

The central and novel finding in the present study is the identification of *in vitro* anticancer efficacy of decursin against advanced human prostate carcinoma DU145, PC-3, and LNCaP cells. The completed studies clearly and convincingly show that decursin causes a G_1 cell cycle arrest via an induction of Cip1/p21 and to a lesser extent Kip1/p27 together with an inhibition in CDK-cyclin kinase activity as an underlying mechanism in its DU145 cell growth inhibition. Furthermore, this agent causes apoptosis induction involving both caspase-dependent and caspase-independent mechanisms in DU145 cells. More importantly, decursin was nontoxic to nonneoplastic human prostate epithelial cells and showed only a moderate cell growth inhibition with a slight effect on cell cycle progression.

The present study also provides an evidence for the structure and anticancer activity of the coumarin compounds decursin and decursinol against hormone refractory human prostate cancer DU145 cells. Based on structural analysis, the side chain in decursin, which is substituted with an -OH group in decursinol (Fig. 1), could be attributed to the enhanced anticancer efficacy of decursin. We also observed that decursinol-caused death of DU145 cells was not associated with apoptosis induction (data not shown); therefore, the substituted side chain in decursin might be solely responsible for its apoptotic efficacy in DU145 cells. Overall, the differential efficacy of these compounds in DU145 cells was in accord with their structure-activity relationship in inhibiting acetylcholinesterase activity reported earlier (18).

CDKs, CDKIs, and cyclins play essential roles in the regulation of cell cycle progression (25). CDKIs are tumor suppressor proteins that down-regulate the cell cycle progression by binding with active CDK-cyclin complexes and thereby inhibiting their kinase activities

decursin were not as effective as higher doses (100 μmol/L) which showed more apoptotic cell death (23%) at 48 hours as compared with 24 hours of treatment (10%) versus controls showing 5% to 8% apoptotic cell death (Fig. 6*A*). These data suggest that apoptosis induction could be a major mechanism of decursin-caused death of prostate cancer cells. With similar decursinol treatment, we did not observe any considerable apoptosis induction in DU145 cells (data not shown).

Role of Caspase Activation in Decursin-Caused Apoptosis. Activation of caspase cascade leading to PARP cleavage is regarded as a major pathway in apoptosis induction (26). Based on the above results showing induction of apoptosis by decursin,

(25, 27, 28). Cip1/p21 is a universal inhibitor of CDKs whose expression is mainly regulated by the p53 tumor suppressor protein (29); however, Kip1/p27 is up-regulated in response to antiproliferative signals (30, 31). The increased expression of G_1 cyclins in cancer cells provides them an uncontrolled growth advantage because most of these cells either lack CDKI, harbor nonfunctional CDKI, or CDKI expression is not at a sufficient level to control CDK-cyclin activity (28, 32). Consistent with these reports, cell cycle analysis data showed that decursin caused a strong G_1 arrest in cell cycle progression of prostate cancer cells. Furthermore, mechanistic investigation showed that decursin-induced G_1 arrest in DU145 cells is mainly mediated via an up-regulation of Cip1/p21 (strong) and Kip1/p27 (moderate). As CDK activity is essential for driving the cells through G_1-S transition (33), concomitant with CDKIs induction, we also observed an increase in Cip1/p21-CDK2/CDK4/CDK6 and Kip1/p27-CDK2/CDK4/CDK6 binding together with an inhibition in CDK-cyclin kinase activity in decursin-treated cells. The increased expression of CDKIs by decursin might also have a direct relevance in prostate cancer growth and progression, as decreased Kip1/p27 expression in prostatic carcinomas has been associated with aggressive phenotype and poor prognosis, and a failure of irradiation response in prostate cancer patients has been linked to the loss of Cip1/p21 function (34). Recent studies have also indicated the prognostic significance of CDKIs in prostate

cancer (35). Specifically, Kip1/p27 expression has been shown to be an independent predictor of prostate-specific antigen failure following radical prostatectomy (36), and its low expression is correlated with poor disease-free survival in prostate cancer patients (37).

Most of the presently available cytotoxic anticancer drugs mediate their effect via apoptosis induction in cancer cells (26, 38), and apoptosis is suggested as one of the major mechanisms for the targeted therapy of various cancers including prostate cancer (26, 38–40). In case of advanced prostate cancer, cancer cells become resistant to apoptosis and do not respond to cytotoxic chemotherapeutic agents (7). Therefore, the agents that induce apoptotic death of hormone-refractory prostate cancer cells could be useful in controlling this malignancy (41). Consistent with this approach, our data showing an induction of apoptotic death of advanced prostate cancer cells by decursin could be of greater significance in identifying another anticancer mechanism (together with cell cycle arrest) of decursin for its possible application in prostate cancer control. Because induction of CDKIs has been reported in anticancer agent–caused apoptosis in human prostate cancer cells (42), the decursin-induced CDKIs could be, in part, responsible for the observed apoptotic death of DU145 cells. The increase in the levels of active caspase-9 and caspase-3 as well as cleaved PARP suggested that caspase activation is another
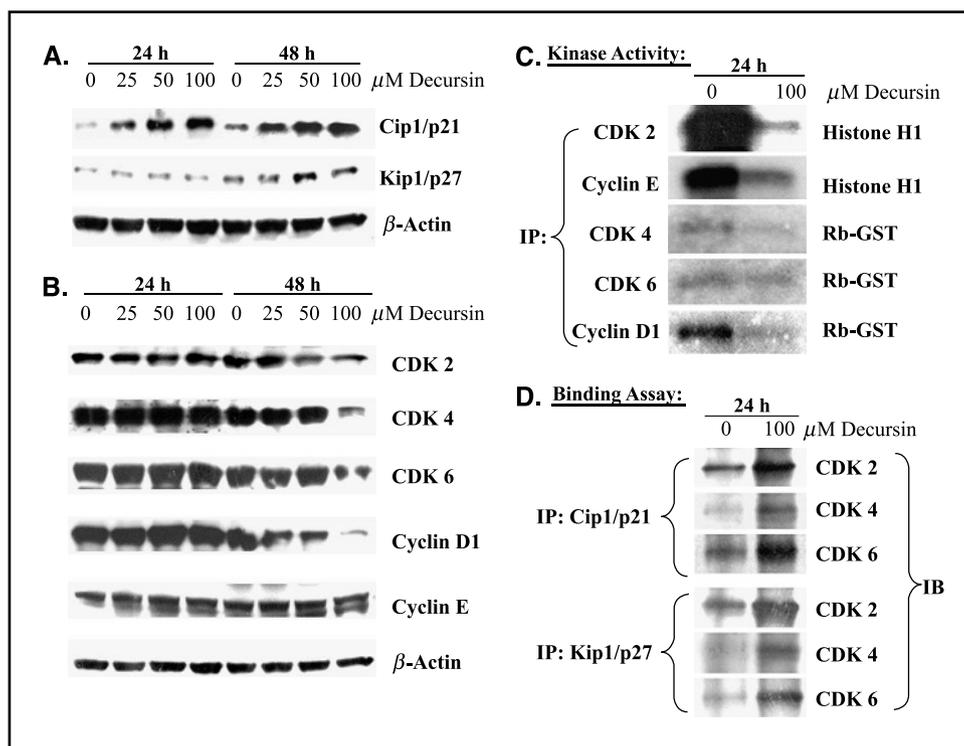
Figure 5. Effect of decursin on G_1 cell cycle regulators and CDK-associated and cyclin-associated kinase activities in DU145 cells. Cells were cultured in complete medium, and treated with either DMSO vehicle control or 25 to 100 μmol/L doses of decursin as described in Materials and Methods. *A* and *B,* at the end of treatments, total cell lysates were prepared and subjected to SDS-PAGE followed by Western immunoblotting. Membranes were probed with anti-Cip1/p21, Kip1/p27, CDK2, CDK4, CDK6, cyclin D1, cyclin E, and β-actin antibodies followed by peroxidase-conjugated appropriate secondary antibodies, and visualized by enhanced chemiluminescence detection system. The experiments were repeated thrice with similar results and a representative blot is shown for each protein. *C,* CDK2 and cyclin E kinase activities were determined by in-bead histone H1 kinase assay using immunoprecipitated CDK2 and cyclin E from total cell lysates (200 μg protein) using specific antibodies. CDK4, CDK6, and cyclin D1-associated kinase activities were determined by in-bead RB-GST fusion protein kinase assay using immunoprecipitated CDK4, CDK6, and cyclin D1 from total cell lysates (200 μg protein) using specific antibodies as described in Materials and Methods. After the assay, the labeled substrates were subjected to SDS-PAGE, and the gel was dried and exposed to X-ray film. *D,* Cip1/p21 and Kip1/p27 were immunoprecipitated using primary specific antibodies, followed by Western blot analysis for CDK2, CDK4, and CDK6 as detailed in Materials and Methods. *IP,* immunoprecipitation; *IB,* immunoblotting.
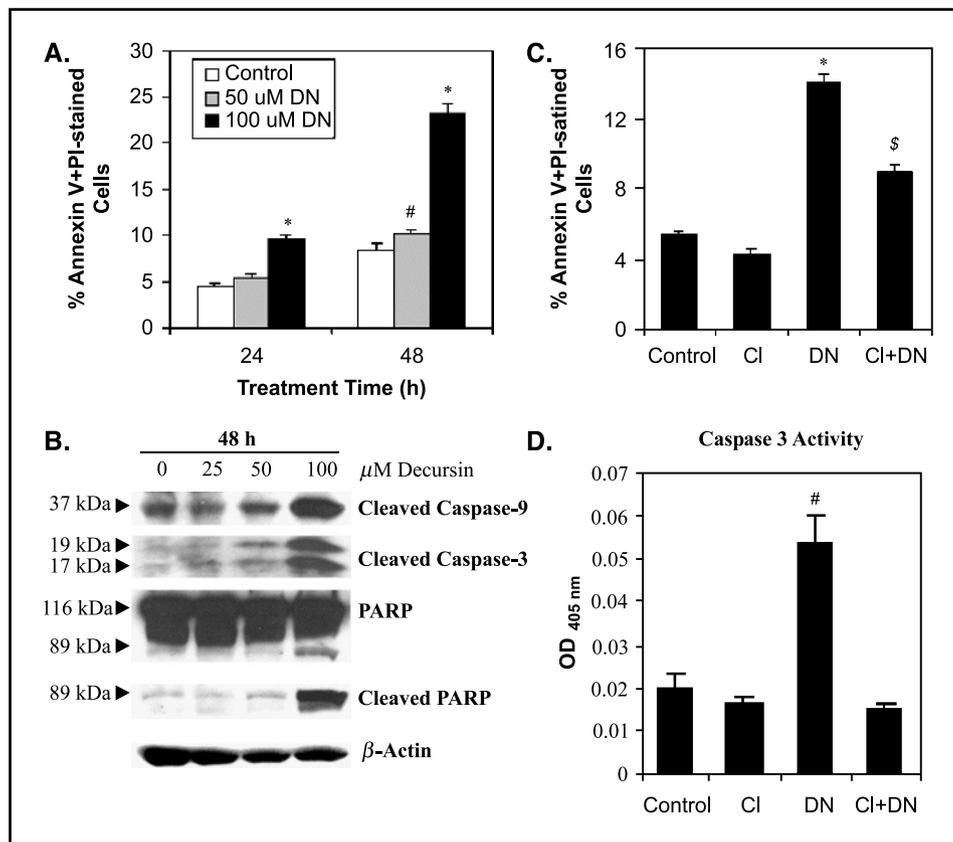
Figure 6. Apoptotic effect of decursin on DU145 cells. *A*, cells were cultured in complete medium, and treated with either DMSO vehicle control or 25 to 100 μmol/L doses of decursin as described in Materials and Methods. At the end of treatments, total cells were collected and stained with annexin V/propidium iodide as mentioned in Materials and Methods followed by flow cytometric analysis. Data are presented as a percentage of annexin V/propidium iodide stained cells for each treatment. *B*, after 48 hours of decursin treatments, cell lysates were prepared and SDS-PAGE and Western blot analysis were performed for cleaved caspase-9, cleaved caspase-3, total and cleaved PARP, and β-actin using specific antibodies as described in Materials and Methods. *C*, cells were cultured in complete medium, and treated with either DMSO vehicle control, 100 μmol/L all-caspases inhibitor (z-VAD-fmk), or 100 μmol/L dose of decursin and/or all caspase inhibitor 2 hours prior to decursin in combination treatment for a total 48 hours. At the end of treatments, cells were analyzed for apoptosis as detailed in Materials and Methods. *D*, in similar treatment as in (*C*), cell lysates were prepared and caspase-3 activity assay was performed as detailed in Materials and Methods. Data presented in (*A*), (*C*), and (*D*) are mean ± SE of three independent samples in each treatment group. *Cl*, 100 μmol/L all caspase inhibitor; *DN*, 100 μmol/L decursin; #, $P < 0.05$; $, $P < 0.01$; *, $P < 0.001$ versus control.

important mechanism in decursin-induced apoptosis in prostate cancer cells. However, use of all-caspases inhibitor also showed the involvement of caspase-independent mechanism(s) in decursin-mediated apoptosis of DU145 cells. Further studies are needed to explore the caspase-independent mechanism(s) of apoptosis induction by decursin.

Several studies suggest that hormone refractory, advanced prostate cancer phenotype is associated with many changes including deregulated cell cycle and cell survival signaling, and inactivation of p53 and pRb such as in DU145 cells. Therefore, findings in the present study have clinical significance in the fact that decursin caused p53-independent up-regulation of Cip1/p21 as DU145 cells do not have functional p53 gene and are also mutated for Rb. Another significant observation was that decursin showed a sustained G_1 arrest in LNCaP cells, which have functional p53 and Rb genes, although this effect was diminished with the increase in treatment time in DU145 and PC-3 cells lacking functional p53 and pRb. This observation suggests the most likely role of p53 and/or pRb in decursin-induced G_1 arrest in LNCaP cells; however, more studies are needed to confirm this anticipation. Furthermore, we also observed that decursin induces S and/or G_2-M arrest at the expense of G_1 phase cell population with the increase in treatment time or at 100 μmol/L dose only in PC-3 cells and not in DU145 or LNCaP cells, suggesting differential molecular determinants of this cell cycle effect of decursin in PC-3 cells.

In conclusion, our present findings showing the *in vitro* anticancer efficacy of decursin, with mechanistic rationale (cell cycle arrest and apoptosis induction), against advanced human prostate cancer cells without any cytotoxicity to nonneoplastic prostate epithelial cells, warrant its further *in vivo* efficacy studies in preclinical human prostate cancer models as well as estimation of pharmacologically achievable doses having biological significance in *in vitro* studies. The positive outcomes of such an *in vivo* study could form a strong basis for the development of decursin as a novel agent for human prostate cancer prevention and/or intervention.

Acknowledgments

References

1. Jemal A, Thomas A, Murray T, et al. Cancer statistics, 2003. CA Cancer J Clin 2003;53:5–26.
2. Bosland MC, McCormick DL, Melamed J, Walden PD, Jacquotte AZ, Lumey LH. Chemoprevention strategy for prostate cancer. Eur J Cancer Chemoprev 2002;11:s18–27.
3. Surh YJ. Cancer chemoprevention with dietary phytochemicals. Nat Rev Cancer 2003;3:768–80.
4. Kelloff GJ, Lieberman R, Steele VE, et al. Chemoprevention of prostate cancer: concepts and strategies. Eur Urol 1999;35:342–50.
5. Feldman BJ, Feldman D. The development of androgen-independent prostate cancer. Nat Rev Cancer 2001;1:34–45.
6. Koivisto P, Kolmer M, Visakorpi T, Kallioniemi OP. Androgen receptor gene and hormonal therapy failure of prostate cancer. Am J Pathol 1998;152:1–9.
7. Pilat MJ, Kamradt JM, Pienta KJ. Hormone resistance in prostate cancer. Cancer Metastasis 1998–99; 17:373–81.
8. Agarwal R. Cell signaling and regulators of cell cycle as molecular targets for prostate cancer prevention by dietary agents. Biochem Pharmacol 2000;60:1051–9.
9. Hong WK, Sporn MB. Recent advances in chemoprevention of cancer. Science 1997;278:1073–7.
10. Kucuk O. Chemoprevention of prostate cancer. Cancer Metastasis Rev 2002;21:111–24.
11. Singh RP, Agarwal R. Prostate cancer prevention by silibinin. Curr Cancer Drug Targets 2004;4:1–11.
12. Giovannucci E. Nutrition, insulin, insulin-like growth factors and cancer. Horm Metab Res 2003;35:694–704.
13. Barnes S. Role of phytochemicals in prevention and treatment of prostate cancer. Epidemiol Rev 2001; 23:102–5.
14. Singh RP, Dhanalakshmi S, Agarwal R. Phytochemicals as cell cycle modulators: a less toxic approach in halting human cancer. Cell Cycle 2002;1:156–61.
15. Nelson PS, Montgomary B. Unconventional therapy for prostate cancer: good, bad or questionable? Nat Rev Cancer 2003;3:845–58.
16. Denmeade SR, Isaacs JT. A history of prostate cancer treatment. Nat Rev Cancer 2002;2:389–96.
17. Chi HJ, Kim HS. Studies on the components of *Umbelliferae* plants in Korea: pharmacological study of decursin, decursinol and nodakenin. Korean J Pharmacog 1970;1:25–32.
18. Kang SY, Lee KY, Sung SH, Park MJ, Kim YC. Coumarins isolated from *Angelica gigas* inhibit acetylcholinesterase: structure-activity relationship. J Nat Prod 2001;64:683–5.
19. Lee S, Shin DS, Kim JS, Oh KB, Kang SS. Antibacterial coumarins from *Angelica gigas* roots. Arch Pharm Res 2003;26:449–52.
20. Ahn KS, Sim WS, Kim IH. Decursin: a cytotoxic agent and protein kinase C activator from the root of *Angelica gigas*. Planta Med 1996;62:7–9.
21. Lee S, Lee YS, Jung SH, Shin KH, Kim BK, Kang SS. Antitumor activity of decursinol angelate and decursin from *Angelica gigas*. Arch Pharm Res 2003;26:727–30.
22. Lee S, Kang SS, Shin KS. Coumarins and pyrimidine from *Angelica gigas* roots. Nat Product Sci 2002;8:58–61.
23. Singh RP, Agarwal C, Agarwal R. Inositol hexaphosphate inhibits growth and induces G$_1$ arrest and apoptotic death of human prostate carcinoma DU145 cells: modulation of CDKI-CDK-cyclin and pRb-related protein-E2F complexes. Carcinogenesis 2003; 24:555–63.
24. Agarwal C, Singh R, Agarwal R. Grape seed extract induces apoptotic death of human prostate carcinoma DU145 cells via caspases activation accompanied by dissipation of mitochondrial membrane potential and cytochrome *c* release. Carcinogenesis 2002;23:1869–76.
25. Grana X, Reddy P. Cell cycle control in mammalian cells: role of cyclins, cyclin-dependent kinases (CDKs), growth suppressor genes and cyclin-dependent kinase inhibitors (CDKIs). Oncogene 1995;11:211–9.
26. Lowe SW, Lin AW. Apoptosis in cancer. Carcinogenesis 2000;21:485–95.
27. Morgan DO. Principles of CDK regulation. Nature (Lond) 1995;374:131–4.
28. Hunter T, Pine J. Cyclins and cancer II: cyclin D and CDK inhibitors come of age. Cell 1994;79:573–82.
29. Xiong Y, Hannon GJ, Zhang H, Casso D, Kobayashi R, Beach D. P21 is a universal inhibitor of cyclin kinases. Nature 1993;366:701–4.
30. Toyoshima H, Hunter T. P27, a novel inhibitor of G$_1$ cyclin-CDK protein kinase activity, is related to p21. Cell 1994;78:67–74.
31. Polyak K, Lee MH, Erdjument-Bromage H, et al. Cloning of Kip1/p27, cyclin-dependent kinase inhibitor and a potential mediator of extracellular antimitogenic signals. Cell 1994;78:59–66.
32. Dulic V, Lees E, Reed SI. Association of human cyclin E with a periodic G$_1$-S phase protein kinase. Science (Washington DC) 1992;257:1958–61.
33. Tsai LH, Lees E, Faha B, Harlow E, Riabowol K. The CDK2 kinase is required for the G$_1$ to S transition in mammalian cells. Oncogene 1993;8:1593–602.
34. Cheng L, Lloyd RV, Weaver AL, et al. The cell cycle inhibitors p21/waf1 and Kip1/p27 are associated with survival in patients treated by salvage prostatectomy after radiation therapy. Clin Cancer Res 2000;6:1896–9.
35. Tsihlias J, Kapusta L, Slingerland J. The prognostic significance of altered cyclin-dependent kinase inhibitors in human cancers. Ann Rev Med 1999;50:401–23.
36. Yang RM, Naitoh J, Murphy M, et al. Low p27 expression predicts poor disease-free survival in patients with prostate cancer. J Urol 1998;159:941–5.
37. Freedland SJ, deGregorio F, Sacoolodge JC, et al. Preoperative p27 status is an independent predictor of prostate specific antigen failure following radical prostatectomy. J Urol 2003;169:1325–30.
38. Gurumurthy S, Vasudevan KM, Rangnekar VM. Regulation of apoptosis in prostate cancer. Cancer Metastasis Rev 2001;20:225–43.
39. Guseva NV, Taghiyev AF, Rokhlin OW, Cohen MB. Death receptor-induced cell death in prostate cancer. J Cell Biochem 2004;91:70–99.
40. Jiang C, Wang Z, Ganther H, Lu J. Caspases as key executors of methyl selenium-induced apoptosis (anoikis) of DU145 prostate cancer cells. Cancer Res 2001;61:3062–70.
41. Kantoff PW. New agents in the therapy of hormone-refractory prostate cancer. Semin Oncol 1995;22:32–4.
42. Don MJ, Chang YH, Chen KK, Ho LK, Chau YP. Induction of CDK inhibitors (p21/waf1 and Kip1/p27) and Bak in the β-lapachone-induced apoptosis of human prostate cancer cells. Mol Pharmacol 2001; 59:784–94.